International Journal of Engineering and Advanced Technology (IJEAT)
ISSN: 2249-8958 (Online), Volume-12 Issue-5, June 2023

Development of Power Conditioning Unit for KY Converter in Fuel Cell Power System

Kanhu Charan Bhuyan, Pushpak Jain, Srutisagar Pattanaik

Abstract: ***The world's growing economy and demographic advancement are driving an increase in global energy demand. As worries about carbon emissions grow and the demand for electrical energy production continues to rise, it is necessary to develop new methods of electricity production. Fuel cell energy system is one of the promising factors for addressing this problem due to its low emissions, easy accessibility, and fuel flexibility. In this paper, a mathematical model of Solid Oxide Fuel Cell (SOFC) is designed and used as an input for the KY converter. As the output voltage of the fuel cell is low, a KY Converter is desired to raise the output voltage for required applications. To regulate the electrical output voltage of the KY Converter, PID, Fuzzy Logic Controller (FLC), hybrid fuzzy PID, and an ANFIS feedback control mechanism have been simulated and investigated. The function of a fuel cell with a KY Converter, as well as state-space modelling, is developed. The Ziegler-Nichols technique is used to determine the gain parameters of a PID controller, which are K_p, K_i, and K_d. The fuel cell with a Closed-loop system of KY converter is developed using MATLAB/Simulink software. Thus, the fuel cell power system can be used for a variety of applications, including rural and military.***

Keywords: Fuel Cell; KY Converter; Controllers, FLC, ANFIS, etc.

I. INTRODUCTION

Energy sources (iron ore, crude oil, and fossil fuels, for example) have led to exponential productivity expansion over the last 200 years, and the world economy continues to heavily depend on them. Nevertheless, a growing concern has been raised about the polluted air, carbon emissions, and global warming affected by such fuels in residential, transport infrastructure, and industrial products. These concerns are the driving force behind a change in thinking toward alternative energy sources with reduced emissions. Solar, wind, ocean, hydro power, and fuel cell resources are projected to provide a more significant amount of energy supply as the world moves toward an emission-free future [1]. Solar and wind contribute a large percentage of sustainable energy. The most significant disadvantage of these renewable resources is their unpredictable existence. Solar is only usable during the day, and the wind is blowing unexpectedly.

Manuscript received on 29 May 2023 | Revised Manuscript received on 05 June 2023 | Manuscript Accepted on 15 June 2023 | Manuscript published on 30 June 2023.

*Correspondence Author(s)
Kanhu Charan Bhuyan*, Department of Electronics & Instrumentation Engineering, OUTR, Bhubaneswar, (Odisha), India. E-mail: kcbhuyan@outr.ac.in, ORCID ID: 0000-0001-8367-397X
Pushpak Jain, Department of Electronics & Instrumentation Engineering, OUTR, Bhubaneswar (Odisha), India. E-mail: pushpakjain58@gmail.com
Srutisagar Pattanaik, Department of Electronics & Instrumentation Engineering, OUTR, Bhubaneswar (Odisha), India. E-mail: srutisagar.pattanaik@gmail.com

Since preserving electrical energy is challenging, excessive green energy can't be saved for longer-term use. So, to mitigate the disadvantage, a fuel cell is used [2]. Fuel cell systems effectively transform the chemical energy released by a fuel oxygen reactant into electrical power. Energy transformation can be more competitive than combustion by electrochemical methods, and, besides, SOFC performs at extreme temperatures, usually 600-1000((C, which allows the reforming of internal fuel. Fuel cell have numerous economic benefits over wind or solar production. They are as follows: high performance at any loading, fuel cells are being installed anywhere in the distribution system, less preservation and higher quality of life negligible carbon emission, and they can also outperform conventional combustion techniques in term of efficiency [3]. Power converters are high frequency power conversion devices that filter out harmonic distortion into controlled DC voltage using high frequency amplification, inductors, and capacitors. The most common circuits are boost, buck, and buck-boost converters, among others. KY Converter is an essential component of the fuel cell unit, this paper presents the modelling of both the fuel cell and the KY converter. The structure of KY converter and their controllers is essential for controlling power management, especially on a distribution substation. The KY converter always operates in Continuous Conduction Mode (CCM) and has a high dynamic transient response rate. The voltage gain is higher than that of several other converters and can also be controlled by changing both the turn's ratio and the duty cycle. A different controlled technique is used in this work to sustain the voltage level of a KY converter in reaction to a continuously shifting fuel cell voltage level and the loads. The simulation of advanced algorithm controllers, such as PID, FLC, Hybrid, and ANFIS controllers, is compared [4]. The remaining part of the paper is divided into four sections, with Section 1 providing a brief introduction. Section 2 presents the operating principle of SOFC with a KY converter. Section 3 describes the different control strategies. Section 4 shows the simulation results along with a comparison table, followed by the brief conclusion in Section 5.

II. SYSTEM COMPONENTS

The block diagram in Figure 1 depicts an FC system that is connected to the KY converter. The module includes several components, including an FC, a DC-DC KY converter, and different controllers. The following part briefly provides an overview of the elements as well as their functions.

2.1. Solid Oxide Fuel Cell (SOFC)

In a fuel cell, hydrogen and oxygen react electrochemically to produce electrical energy in a static system. To depict the dynamic and static reactions of the fuel cell, the design reflects the effect of all errors throughout the fuel cell and applies the essential electrochemical equations with their respective corresponding electrical components. The system is independent of the fuel cell's physical form and can be easily applied to model fuel cell stacks [5].

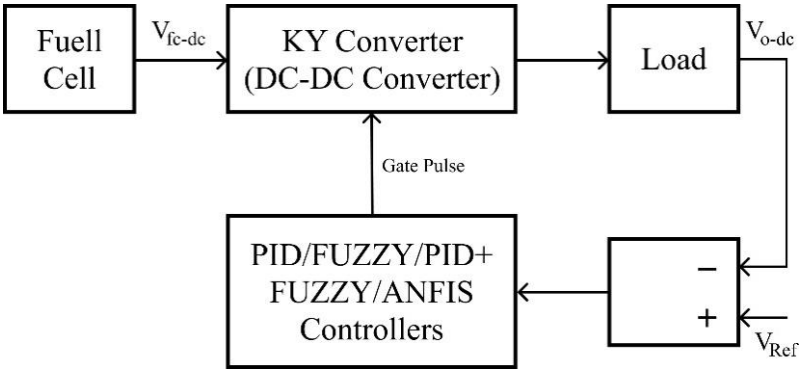

Fig. 1. Block diagram of fuel cell system with converter.

The following equations represent the electrode reaction:

$$\text{Anode}: H_2 + O^{2-} \rightarrow H_2O + 2e^- \quad (1)$$

$$\text{Cathode}: \frac{1}{2}O_2 + 2e^- \rightarrow O^{2-} \quad (2)$$

After Combining the equation (1) and (2) the overall reaction is given as,

$$\text{Reaction}: H_2 + \frac{1}{2}O_2 \rightarrow H_2O \quad (3)$$

Hydrogen gas reacts with oxygen ions at the anode to create gaseous water, and electrons are released as a source of electrical energy. Oxygen interacts with the electrons collected from the electrode at the cathode, resulting in oxygen ions [2].

A connection given below describes the voltage output of the fuel cell that uses fuel and air as its reactant:

$$V_{fc-dc} = E_{nernst} - V_{act} - V_{ohm} - V_{conc} \quad (4)$$

Where,

V_{fc-dc} is the output voltage of SOFC (Volts)

E_{nernst} is the Nernst voltage (Volts)

V_{act} is the activation of voltage drop

V_{ohm} is the ohmic voltage drop

V_{conc} is the concentration of voltage drop

As below, known Nernst formula is used to calculate the open-circuit electromotive force of a stack of N_o cells in sequence.

$$E_{nernst} = E_0 + \frac{RT}{2F}\ln\left(\frac{P_{H2}P_{O2}^{0.5}}{P_{H2O}}\right) \quad (5)$$

Where,

E_0 is the voltage of reaction free energy (1.1V)

R is the universal gas constant ($8.31\, joule.mol^{-1}K^{-1}$)

T is the operating temperature of SOFC

F is the faraday constant (96487C/mol)

$P_{H_2}, P_{O_2}, P_{H_2O}$ are hydrogen, oxygen and water partial pressures, respectively.

The equations regarding $P_{H_2}, P_{O_2}, P_{H_2O}$ is given as:

$$P_{H2} = \left(\frac{\frac{1}{K_{H2}}}{1+\tau_{H2}} \right) \left(q_{H2} - 2K_r I_{fc} \right) \quad (6)$$

$$P_{O2} = \left(\frac{\frac{1}{K_{O2}}}{1+\tau_{O2}} \right) \left(q_{O2} - 2K_r I_{fc} \right) \quad (7)$$

$$P_{H2O} = \left(\frac{\frac{1}{K_{H2O}}}{1+\tau_{H2O}} \right) \left(2K_r I_{fc} \right) \quad (8)$$

$$q_{H2} = \frac{2K_r}{U_{opt}} \left(\frac{1}{1+\tau_f s} \right) \quad (9)$$

$$q_{O2} = \frac{q_{H2}}{r_{OH}} \quad (10)$$

Where, q_{H_2} flow rate of fuel, q_{O_2} flow rate of oxygen, $K_{H_2}, K_{O_2}, K_{H_2O}$ the hydrogen, oxygen, and water molar value constants, respectively, $\tau_{H_2}, \tau_{O_2}, \tau_{H_2O}$ are the hydrogen, oxygen, and water response times, respectively, τ_f is the time it takes for the fuel to respond in seconds, U_{opt} is the most effective use of fuel, and r_{OH} is the hydrogen to oxygen ratio.

The energy necessary to achieve the energy constraints for the chemical reaction to commence is referred to as "activation loss" [6]. The activation losses on the anode and cathode sides are provided by:

$$I_{fc} = I_O \left(e^{(\alpha_1 F/RT)V_{act}} - e^{(\alpha_2 F/RT)V_{act}} \right) \quad (11)$$

$$V_{act} = \frac{RT}{n\alpha F} \ln \left(I_{fc}/2I_O + \sqrt{(I_{fc}/2I_O)^2 + 1} \right) \quad (12)$$

Meanwhile, the concentration polarization loss induced by the oxygen and hydrogen gases' failure to disperse quickly enough during the cell's porous constituents is given by [6].

$$V_{conc} = -\frac{RT}{nF} \ln \left(1 - \frac{I_{fc}}{I_L} \right) \quad (13)$$

The influx of electrolyte, as well as the flow of electrons across the electrodes, would often encounter resistance. Both defeats add up to an ohmic loss. The cell's intrinsic resistance varies with temperature and is calculated using the equation [6].

$$V_{ohmic} = \left(\gamma \exp \left[\beta \left(\frac{1}{T_O} - \frac{1}{T} \right) \right] \right) I_{fc} = rI_{fc} \quad (14)$$

Where, $T_O = 973K$, T is the temperature coefficient of the fuel cell, and r is the internal resistance, $\gamma = 0.2\Omega$ *and* $\beta = -2870K$ are the static coefficients of the fuel cell.

2.2. KY Converter

KY converter that uses to boost the output voltage same as the other converters. The PWM gate pulse is provided to the MOSFET, this operates the MOSFETs in the circuit. This converter has two switching MOSFETs Q1 and Q2 along with their parasitic diodes d1 and d2 [7,8]. It also contains one return inductor L_0, one return capacitor C_0, and one energy transferring capacitor C_b. The KY converter is shown in Figure 2. The inductor stores the energy when switch Q1 is halted and switch Q2 is in open condition, and this energy is in the form of magnetic energy. The inductor discharges this energy when switch Q1 is open and switch Q2 is closed.

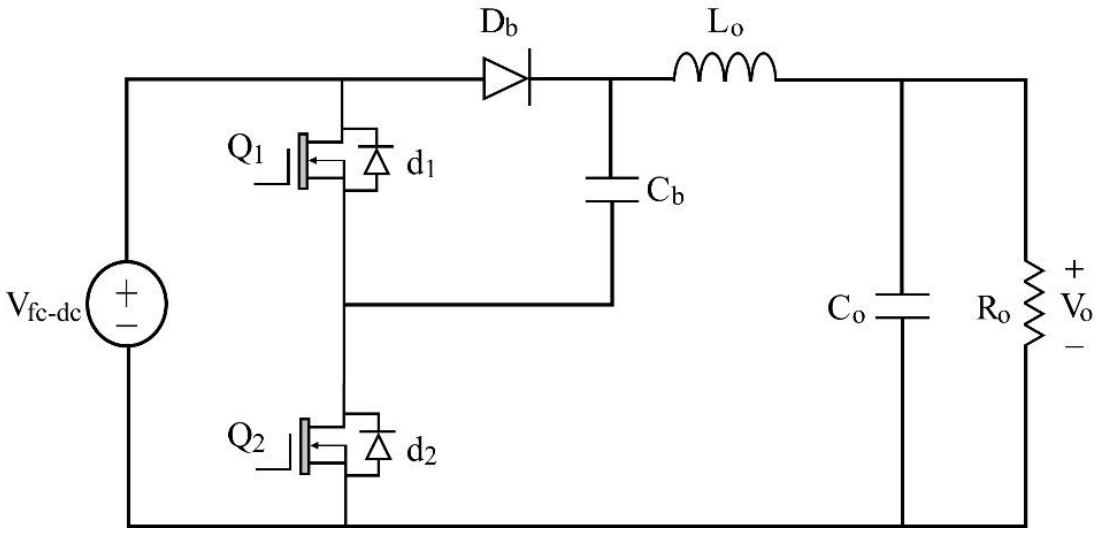

Fig. 2. Circuit diagram of KY Converter [4].

2.2.1 Mode-1

When the PWM is applied to the gate drive of both MOSFETS, then the switch Q1 is in ON state due to high gate signal and switch Q2 is in off state due to low gate signal. In this mode, the voltage across the N side of the diode is much higher than the P side due to this diode behaves as an open circuit. The time in which the circuit operates is T_{ON} second. During this time, it charges the inductor and the current of the inductor increases which makes the inductor magnetized. The mode-1 of the KY converter is shown in Figure 3 [9].

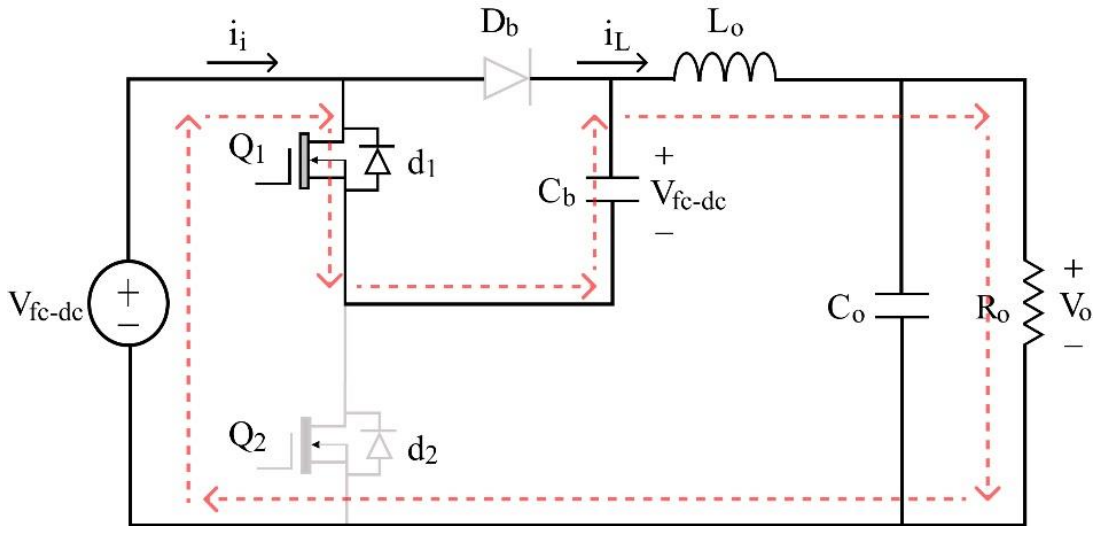

Fig 3. KY converter during mode-1 [4].

Here the duty cycle is,

$$D = \frac{T_{ON}}{T} \tag{15}$$

From equation (15), we get

$$T_{ON} = D * T \tag{16}$$

By using KVL the differential equation is given as,

$$V_{LO} = V_{fc-dc} + V_{Cb} - V_O \tag{17}$$

Where the voltage across the energy transferring capacitor C_b is same as input voltage V_s, so

$$V_{LO} = 2V_{fc-dc} - V_O \tag{18}$$

Retrieval Number:100.1/ijeat.E41990612523
DOI: 10.35940/ijeat.E4199.0612523
Journal Website: www.ijeat.org

Published By:
Blue Eyes Intelligence Engineering and Sciences Publication (BEIESP)

$$L\frac{\partial i}{\partial t} = 2V_{fc-dc} - V_O \quad (19)$$

$$i_{Co} = i_L - i_O \quad (20)$$

$$C\frac{\partial v_o}{\partial t} = i_L - \frac{V_O}{R} \quad (21)$$

From equation (19 and 21) the state space model for Mode-1 is given as,

$$\begin{bmatrix} i_L \\ v_C \end{bmatrix} = \begin{bmatrix} 0 & \frac{-1}{L} \\ \frac{1}{C_O} & \frac{-1}{R_O C_O} \end{bmatrix} \begin{bmatrix} i_L \\ v_C \end{bmatrix} + \begin{bmatrix} \frac{2}{L} \\ 0 \end{bmatrix} \begin{bmatrix} V_{fc-dc} \end{bmatrix} \quad (22)$$

$$Y_0 = \begin{bmatrix} 1 & 1 \end{bmatrix} \begin{bmatrix} i_L \\ V_C \end{bmatrix} \quad (23)$$

2.2.2 Mode-2

In this mode, switch Q1 is in off state due to low gate signal, and switch Q2 is in ON state due to high state signal. In this mode, the voltage across the N side of the diode is lower than the P side due to this diode behaves as a short-circuit. The time in which the circuit operates is T_{OFF} second. During this time, the inductor will discharge through the capacitor C_b and the output combination $R_O C_O$. The mode-2 of KY converter is shown in Figure 4 [9].

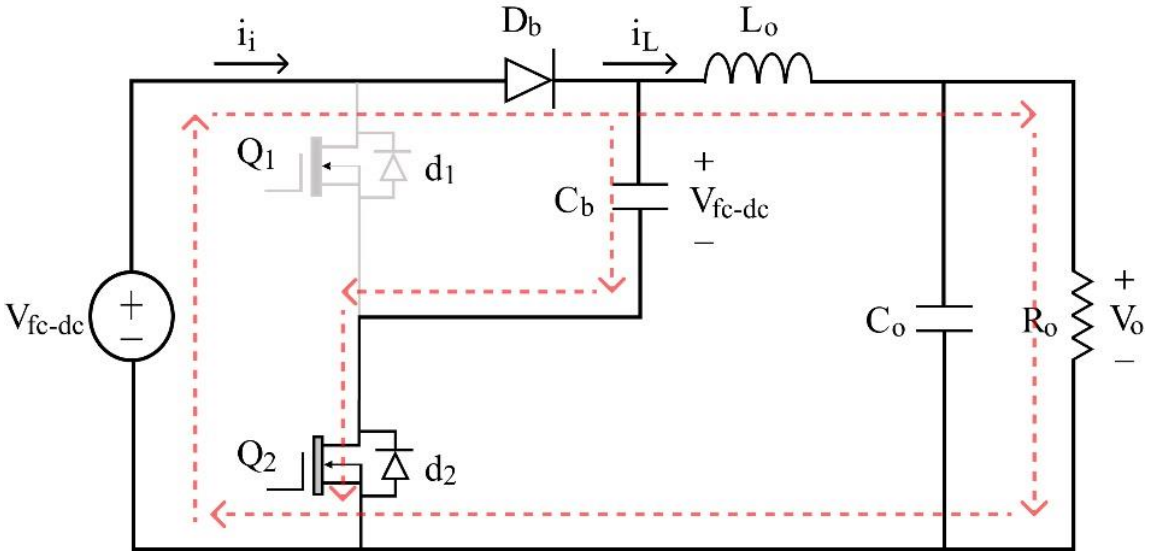

Fig 4. KY converter during mode-2 [4].

Here the duty cycle is,

$$1 - D = \frac{T_{ON}}{T} \quad (24)$$

From equation (24), we get

$$T_{OFF} = (1 - D) * T \quad (25)$$

By using KVL the differential equation is given as,

$$V_{LO} = 2V_{fc-dc} - V_O \quad (26)$$

$$L\frac{\partial i}{\partial t} = V_{fc-dc} - V_O \quad (27)$$

$$i_{Co} = i_L - i_O \quad (28)$$

$$C\frac{\partial v_o}{\partial t} = i_L - \frac{V_O}{R} \quad (29)$$

From equation (27 and 29) the state space model for Mode-1 is given as,

$$\begin{bmatrix} i_L \\ v_C \end{bmatrix} = \begin{bmatrix} 0 & \frac{-1}{L} \\ \frac{1}{C} & \frac{-1}{R_O C_O} \end{bmatrix} \begin{bmatrix} i_L \\ v_C \end{bmatrix} + \begin{bmatrix} \frac{1}{L} \\ 0 \end{bmatrix} \begin{bmatrix} V_{fc-dc} \end{bmatrix} \quad (30)$$

$$Y_0 = \begin{bmatrix} 1 & 1 \end{bmatrix} \begin{bmatrix} i_L \\ V_C \end{bmatrix} \quad (31)$$

2.3. Small Signal Analysis and Averaging

The average large signal model can be found out by using the state space matrices of Mode-1 and Mode-2 that is expressed in equation (22 and 23) and (30 and 31)

$$A = A_{ON} \times (D) + A_{OFF} \times (1-D) \quad (32)$$

$$B = B_{ON} \times (D) + B_{OFF} \times (1-D) \quad (33)$$

$$C = C_{ON} \times (D) + C_{OFF} \times (1-D) \quad (34)$$

Where system matrices are A_{ON} *and* A_{OFF}, input matrices are B_{ON} *and* B_{OFF}, output matrices are C_{ON} *and* C_{OFF}. The average equation of KY converter is given as:

$$\dot{X} = AX + BV_{fc-dc} \quad (35)$$

$$\dot{Y} = CX + DU \quad (36)$$

Where,

$$A = \begin{bmatrix} 0 & \frac{-1}{L} \\ \frac{1}{C} & \frac{-1}{R_O C_O} \end{bmatrix} \quad (37)$$

$$B = \begin{bmatrix} \frac{1+D}{L} \\ 0 \end{bmatrix} \quad (38)$$

$$C = \begin{bmatrix} 1 & 1 \end{bmatrix} \quad (39)$$

The final transfer function can be calculated as,

$$Y(s) = C\left(sI - A\right)^{-1} B + D \quad (40)$$

$$Y(s) = \frac{\left(RC + RCD\right)s + R + RD + 1 + D}{RLC_0 s^2 + Ls + R} \quad (41)$$

III. CONTROL METHODS

A controller that gets input from the plant, may get the set point or reference point from the outer source and cycle this data so that plant will act in the way as expected by the reference.

3.1. PID Controller

The PID control method is the most famous response controller. In terms of industry, a control method is a required component. The PID controller algorithm can be defined by:

$$u(t) = K\left(e(t) + \frac{1}{Ti} \int_0^t e(\tau)\partial\tau + T_d \frac{\partial e(t)}{\partial t} \right) \quad (42)$$

The P-term, I-term, and the D-term are the three words that make up the control structure. Where the P represent the inaccuracy, the I represent the integral of the inaccuracy, and D represent the derivative of the inaccuracy.

The frequency response approach developed by Ziegler and Nichols has been used to access the value of PID. To further calculate the value of K_P, K_I *and* K_D, the two important values that has taken into account are the ultimate gain ($K_u = 1/K_{180}$) and the ultimate period ($T_u = 2\Pi/\omega_{180}$).

After putting the value of Table 4 in the equation 41, we get K_u as 0.53 and Tu as 309, from Ku and T_u, T_i and T_d can be calculated as:

$$T_i = 0.5 \times T_u = 0.5 \times 309 = 154.5 \quad (43)$$

$$T_d = 0.125 \times T_u = 0.125 \times 309 = 38.62 \quad (44)$$

This gives Ti as 154.5 and Td as 38.625

$$K_p = 0.6 \times K_u = 0.6 \times 0.53 = 0.318 \quad (45)$$

$$K_i = \frac{K_p}{T_i} = \frac{0.318}{154.5} = 0.0020 \quad (46)$$

$$K_d = K_p \times T_d = 0.318 \times 38.625 = 12.28 \quad (47)$$

This gives K_p as 0.318, Ki as 0.0020, and K_d as12.28.

3.2. Fuzzy Logic Controller

For linear systems, PID controllers are used. Their output is impaired by the existence of nonlinear effects. Along with their knowledge based nonlinear attributes and ability to manage vast quantities of data, fuzzy controllers are popular in nonlinear systems [10].

Table 1. Fuzzy controller rule base.

E/CE	NB	NS	ZE	PS	PB
PB	NS	NB	PB	PB	PS
PS	NS	NS	PS	PS	PS
ZE	ZE	ZE	ZE	ZE	ZE
NS	PS	PS	NS	NS	NS
NB	PS	PB	NB	NB	NS

The inaccuracy and the change in inaccuracy are the two input parameters for the Mamdani fuzzy inference system, with output1 as the output variable [11]. The input and output variables have a vector set value of 3. The total number of rules that are defined in the rule base is 25(5X5) as shown in Table 1.

3.3. Hybrid Controller (FLC+PID)

The hybrid controller is a combination of fuzzy logic controller and PID. PID controller can't solve all control issues. In general, the process involved is complicated and time variant, with disruptions and non-linearity, and frequently has imprecise dynamics. FLC aids in the translation of heuristic knowledge as well as control procedures into mathematical models. It is more efficient than the other controllers. These controllers use rate information and the error of the system response together [12,13].

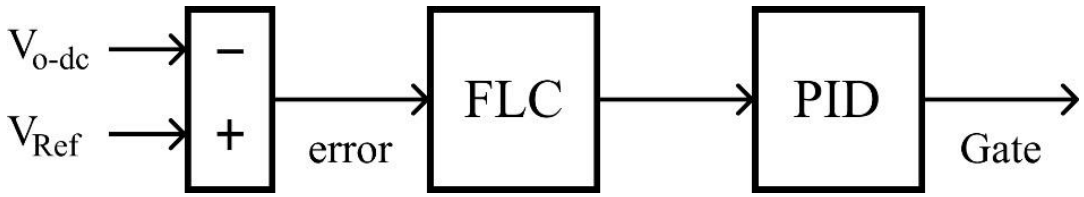

Fig 5. Block diagram of hybrid controller.

Table 2. Hybrid controller rule base.

E/CE	NB	NS	ZE	PS	PB
NB	PS	PB	NB	NB	NS
NS	PS	PS	NS	NS	NS
ZE	ZE	ZE	ZE	ZE	ZE
PS	NS	NS	PS	PS	PS
PB	NS	NB	PB	PB	PS

The primary fuzzy set rule, such as positive small, positive big, zero, negative small, and negative big has been used. The total number of rules that are defined in the rule base is 25(5X5) as shown in Table 2. The performance would be positive small if the change of error is positive big and the error is positive small.

3.4. ANFIS Controller

The rule base in FLC is not fixed; it varies from expert to expert. Creating the rule base necessary involves expert knowledge [14]. This disadvantage is overcoming by ANFIS. Because ANFIS is a hybrid of a neural network and a fuzzy logic controller, no specialist knowledge is required to build a rule base.

Published By:
Blue Eyes Intelligence Engineering
and Sciences Publication (BEIESP)

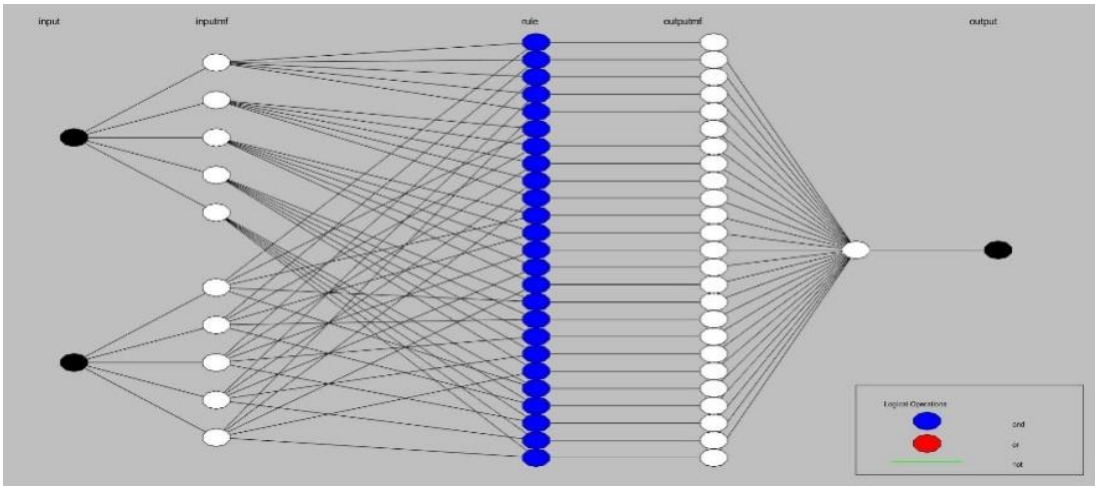

Fig 6. ANFIS model structure.

Table 3. ANFIS controller rule base.

E/CE	In2mf1	In2mf2	In2mf3	In2mf4	In2mf5
In1mf1	Out1mf1	Out1mf2	Out1mf3	Out1mf4	Out1mf5
In1mf2	Out1mf6	Out1mf7	Out1mf8	Out1mf9	Out1mf10
In1mf3	Out1mf11	Out1mf12	Out1mf13	Out1mf14	Out1mf15
In1mf4	Out1mf16	Out1mf17	Out1mf18	Out1mf19	Out1mf20
In1mf5	Out1mf21	Out1mf22	Out1mf23	Out1mf24	Out1mf25

The ANFIS model structure is shown in Figure 6 having two inputs in1 and in2 with one output out1. The rule base is developed using "and" operator [15]. The performance would be out1mf1 if the error is in1mf1 and the change of error is in2mf1. A membership function of the shape of a triangle is taken. The total number of the rules that is defined in the rule base is 25(5X5) as shown in Table 3.

IV. SIMULATION RESULTS AND ANALYSIS

The fuel cell is regulated in the allowable range of 12 to 16 volts for constant fuel supply to ensure the system's stability. The MATLAB/Simulink software is used to simulate the SOFC with closed loop feedback KY boosting converter. This converter controls the output of fuel cell voltage and increases the efficiency of the SOFC system. Figure 7 shows that the fuel cell voltage takes about 0.30 ms to achieve a steady state and 0.202 ms to reach the acceptable voltage level.

Table 4. Parameters of fuel cell with KY converter.

Parameters	Rating
Fuel cell voltage	12 – 16V
Converter output voltage	18V
Energy transferring capacitor	100µF
Output capacitor	1000µF
Output inductor	4.7µH
Power	50W
Load	4 Ω

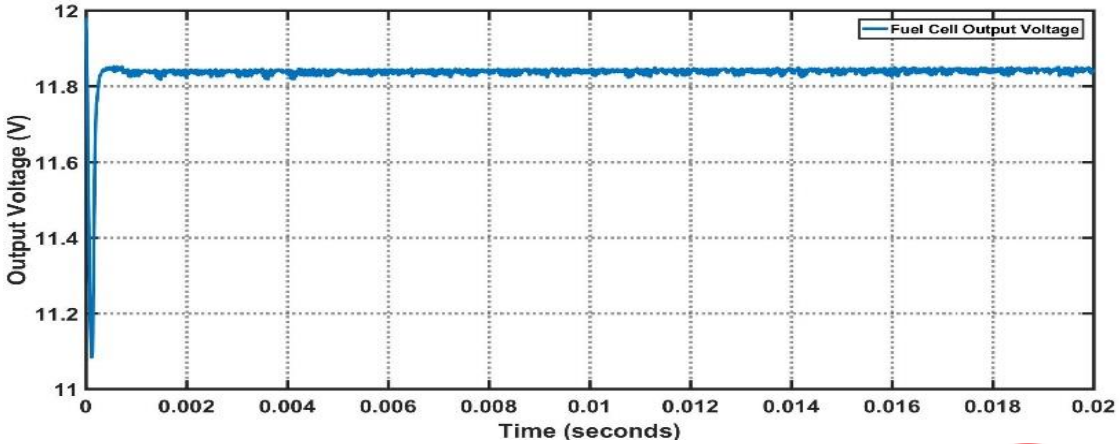

Fig 7. Fuel cell output voltage.

Published By:
Blue Eyes Intelligence Engineering
and Sciences Publication (BEIESP)

The comparison of KY converter with SEPIC and Buck-Boost is tabulated and is shown in Table 5. The KY converter is settled in time of 1.26 ms with the efficiency of 90.92% and having the 0.3104 V amount of voltage ripple, which is very less than the other converters.

Table 5. Comparison of converters

Parameters	Buck-Boost	SEPIC	KY
I/P Voltage ($V_{fc\text{-}dc}$)	12V	12V	12V
O/P Voltage ($V_{O\text{-}dc}$)	17.32V	17.52V	17.73V
Settling time (s)	2.01ms	6.49ms	1.26ms
Rise time (s)	72.6µs	78.9µs	70µs
Voltage ripple (V)	0.3868	0.4297	0.3104
Efficiency	86.3	88.61	90.92

The output voltage of KY converter using PID controller is stabilized in 1.196 ms and 0.0757 ms to meet the appropriate voltage stage, with a significant overshoot of 17.09% and a lower efficiency of 82.28% as compared to other controllers are shown in Figure 8.

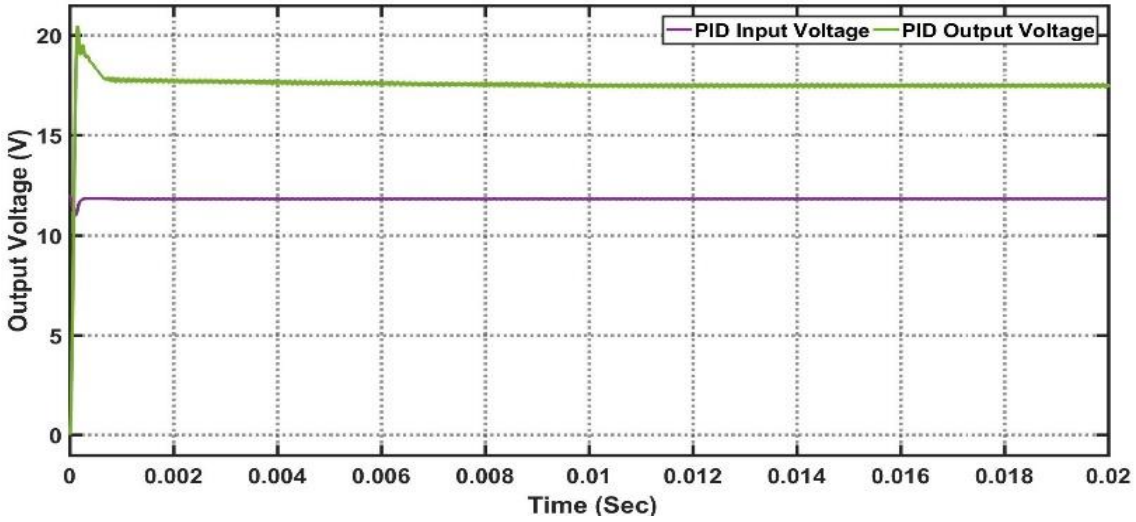

Fig 8. Output of KY converter with PID controller.

In comparison to other controls, the output voltage of KY converter using a FLC is stabilized in 0.7778 ms and 0.0745 ms to achieve the required voltage level, with a large overshoot of 18.52% and a higher efficiency performance of 90% as shown in Figure 9.

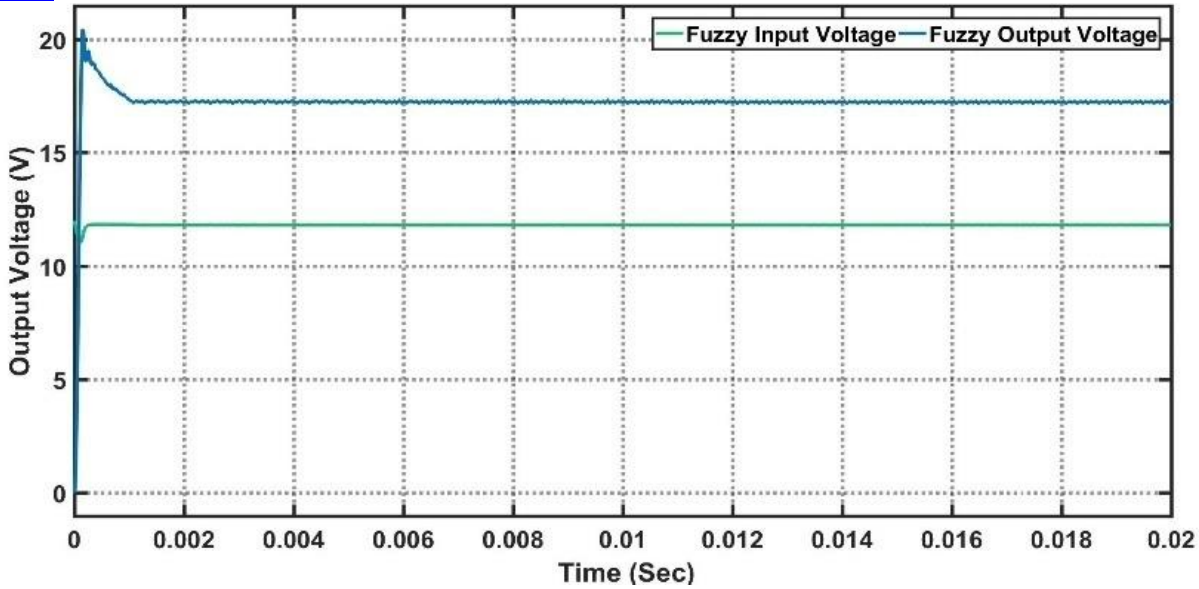

Fig 9. Output of KY converter with fuzzy logic controller.

The output voltage of KY converter using a Hybrid controller is stable in 0.518 ms and 0.076 ms to reach the required voltage level, as seen in Figure 10, with a less overshoot of 15.69% as compared to PID and fuzzy controller and having an efficiency performance of 89%.

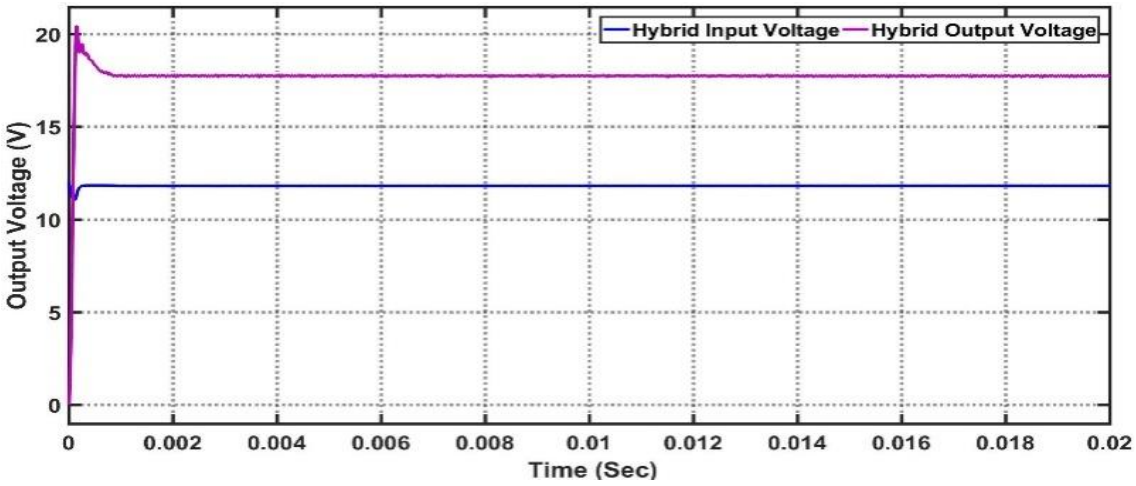

Fig 10. Output of KY converter with hybrid controller.

As compared to other controllers, the ANFIS controller will settle the output voltage within 0.223 ms and take 0.076 ms to reach the required voltage level with very little overshoot which is 11.79%, and having an efficiency performance of 84% shown in Figure 11.

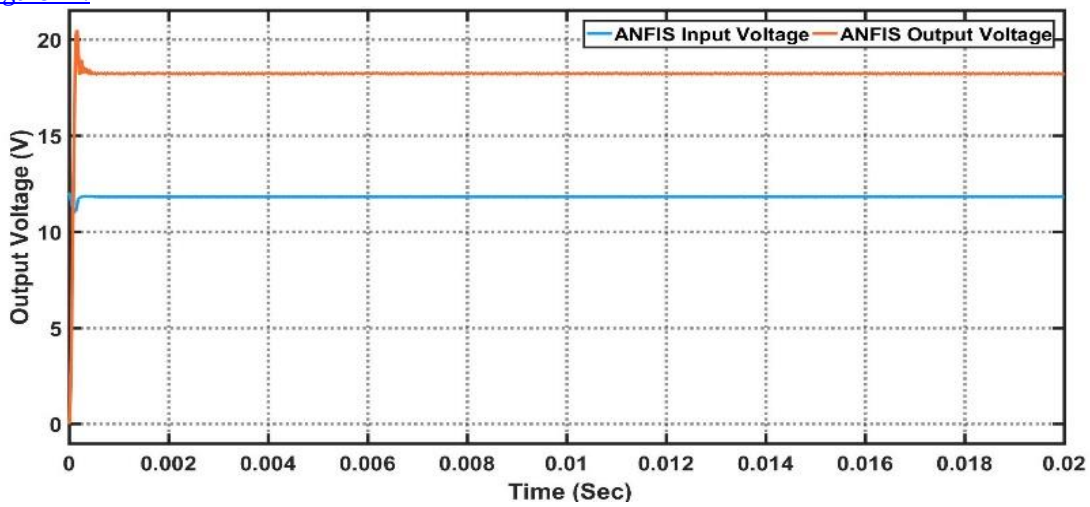

Fig 11. Output of KY converter with ANFIS controller.

The output voltage of KY converter using various feedback control techniques is shown in Figure 12, where ANFIS demonstrates a stronger performance with less overshoot and settled efficiency to a steady output voltage with an expected range of efficiency.

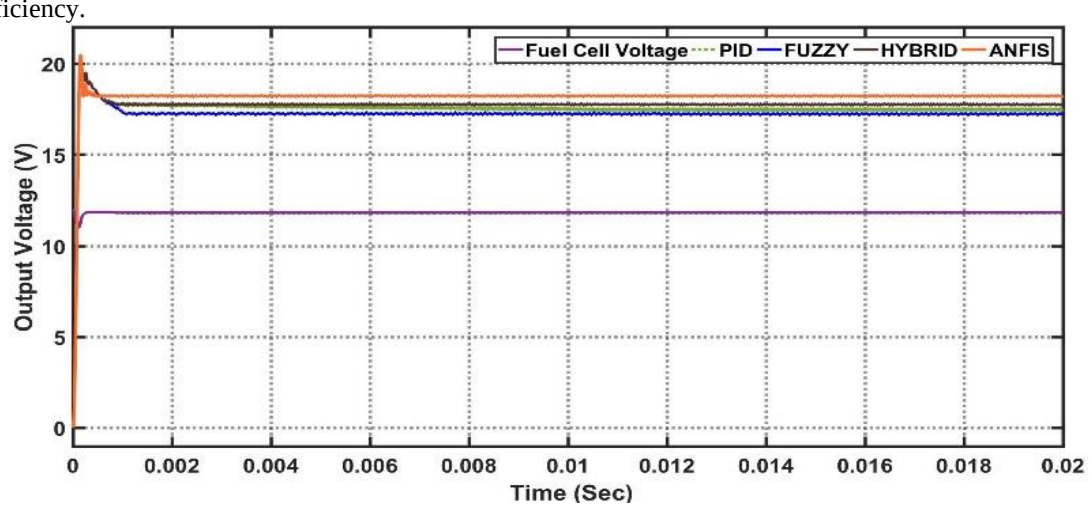

Fig 12. Output of KY converter with controllers.

Table 6. Comparison of controllers

Parameters	PID	FLC	HYBRID	ANFIS
I/P Voltage ($V_{fc\text{-}dc}$)	12V	12V	12V	12V
O/P Voltage ($V_{O\text{-}dc}$)	17.61V	17.23V	17.76V	18.28V
Settling time (s)	1.196ms	778.8µs	518µs	223µs
Rise time (s)	75.78µs	74.5µs	76µs	76µs
Overshoot	17.09	18.52	15.69	11.79
Efficiency	82.28	90	89	86

Table 6 shows the comparison of different controllers at a constant load, where the ANFIS controller does have a better settling period, overshoot, and rise time.

Table 7. PID controller at various input voltage.

I/P Voltage	O/P Voltage	Settling Time	Rise Time	Overshoot
12 V	17.09V	1.541ms	77.6µs	18.69
13 V	17.23V	1.98ms	74.8µs	23.70
14 V	18.34V	2.55ms	72.4µs	38.87
15 V	18.36V	3.65ms	70µs	44.98
16 V	18.34V	7.19ms	67.92µs	50.64

Table 7 shows the PID controller, and how the settling time and output voltage increased as the input voltage is increased, with a large amount of overshoot and rise time, having high fluctuation in comparison to other controllers.

Table 8. Fuzzy logic controller at various input voltage.

I/P Voltage	O/P Voltage	Settling Time	Rise Time	Overshoot
12 V	17.19V	665µs	74.2µs	18.45
13 V	17.52V	875µs	69.94µs	25.94
14 V	17.55V	1.131ms	66µs	34.45
15 V	17.71V	1.344ms	64µs	42.14
16 V	17.77V	1.676ms	61.8µs	50.75

Table 8 shows the input voltage is increased in a FLC, the settling time is increased which is less than the PID controller and having the consistent output voltage, with a high overshoot and having high error in comparison to Hybrid and ANFIS controllers.

Table 9. Hybrid controller at various input voltage.

I/P Voltage	O/P Voltage	Settling Time	Rise Time	Overshoot
12 V	17.73V	469µs	76µs	15.69
13 V	17.8V	698µs	71.5µs	22.84
14 V	17.83V	1.040ms	67µs	32.66
15 V	17.88V	1.280ms	64µs	40.14
16 V	17.92V	1.536ms	61.4µs	48.50

Table 9 shows as the input voltage is increases in a hybrid controller, the settling time is increased which is less than the PID and fuzzy controller and having the consistent output voltage and less rise time, with a less overshoot and having less error as compared to PID and fuzzy controllers.

Table 10. ANFIS controller at various input voltage.

I/P Voltage	O/P Voltage	Settling Time	Rise Time	Overshoot
12 V	18.16V	184.5µs	78.5µs	11.80
13 V	18.18V	534.6µs	73µs	19.88
14 V	18.19V	849µs	68µs	29.2
15 V	18.21V	1.128ms	65µs	36.3
16 V	18.22V	1.34ms	62µs	44

ANFIS controller offers minimum amount of settling time, rise time and overshoot with a constant output voltage as the input voltage is increased. This controller has a better response than the other controllers and has a very low error rate, as shown in Table 10.

V. CONCLUSIONS

Fuel cell with KY converter using different control strategies are simulated in MATLAB. The KY converter has been compared to the SEPIC and Buck-Boost converters, with the output settling in 1.26 ms, shortened output voltage ripple, rapid transient responses, and high efficiency of 90.92%. the system is simulated with various control techniques and determining that the settling time of the fuel cell system using ANFIS controller is very short with a time of 0.223 ms, a low amount of overshoot 11.79% is within the predicted efficiency range. Further, the system simulated with varying input voltages (12-16V), and it is observed that the HYBRID and ANFIS controller have stable performance. The simulating results of various controlled techniques such as PID, FLC,

Published By:
Blue Eyes Intelligence Engineering
and Sciences Publication (BEIESP)

HYBRID, and ANFIS are tabulated in terms of settling time, rise time, and overshoot, and it is concluding that the ANFIS controller is the best at stabilizing the output voltage with the fewest number of iterations.

DECLARATION

Funding/ Grants/ Financial Support	Yes, This work is funded by Odisha State Higher Education Council, OURIIP-2020
Conflicts of Interest/ Competing Interests	No conflicts of interest to the best of our knowledge.
Ethical Approval and Consent to Participate	No, the article does not require ethical approval and consent to participate with evidence.
Availability of Data and Material/ Data Access Statement	Not relevant.
Authors Contributions	All authors have equal participation in this article

REFERENCES

1. Khojasteh; Danial; davood Khojasteh; Reza Kamali; Asfaw Beyene; Gregorio Iglesias. Assesment of renewable energy resources in Iran; with a focus on wave and tidal enrgy. Renewable and Sustainable Energy Reviews 2018, 81, 2992-3005. [CrossRef]
2. Rath; Prabodha Kumar; Kanhu Charan Bhuyan. Vector Control of Fuel Cell Based Grid Connected Inverter. Journal of Green Engineering 2018, 8(3), 201-218. [CrossRef]
3. Sun; Li; Guiying Wu; Yali Xue; Jiong Shen; Donghai Li; Kwang Y.Lee. Coordinated control strategies for fuel cell power plant in a microgrid. IEEE Transaction on Energy Conversion 2017, 33(1), 1-9. [CrossRef]
4. K. I. Hwu; Y. T. Yau. KY Converter and Its Derivatives. IEEE Transaction on Power Electronics 2009, 24(1), 128-137 [CrossRef]
5. Gebregergis; Abraham; Pragasen Pillay. The development of solid oxide fuel cell (SOFC) emulator. IEEE Power Electronics Specialists Conference 2007, 1232-1238. [CrossRef]
6. Sirisukprasert; Siriroj; Trin Saengsuwan. A novel power electronics-based fuel cell emulator. ECTI Transaction on Electrical Engineering, Electronics, and Communications 2009, 7(2), 63-71 [CrossRef]
7. Ohta; Yoshihiro; Kohji Higuchi; T. Kajikawa. Robust Digital Control for Boost DC-DC Converter. ECTI Transactions on Electrical Engineering, Electronics, and Communications 2011, 10(1), 68-73. [CrossRef]
8. G. Saritha; D. Kirubakaran. Design and Implementation of KY Buck-Boost Converter with Voltage Mode Control. IJEAT 2019, 8(5), 527-531.
9. Kanhu Charan Bhuyan; Rajesh Kumar Patjoshi; Subhransu Padhee; Kamalakanta Mahapatra. Solid Oxide Fuel Cell with DC-DC Converter System: Control and Grid Interfacing. WSEAS Transaction on Systems and Control 2014, 9.
10. Panigrahi; Anwesha; Kanhu Charan Bhuyan. Fuzzy Logic Based Maximum Power Point Tracking Algorithm for Photovoltaic Power Generation System. Journal of Green Engineering 2016, 6(4), 403-426.
11. Pushpavalli M; Jothi Swaroopan NM. KY converter with fuzzy logic controller for hybrid renewable photovoltaic/wind power system. Transaction on Emerging Telecommunications Technologies 2020, 31(12), e3989. [CrossRef]
12. Lee; Chuen-Chien. Fuzzy logic in control system: fuzzy logic controller. IEEE Transaction on systems, man, and cybernetics 1990, 20(2), 404-418. [CrossRef]
13. Cirstea M; Dinu A; McCormick M; Khor JG. Neural and fuzzy logic control of drives and power systems, 1st ed.; Elsevier; 2002; pp.1-399. [CrossRef]
14. Wu; Tiezhou; Mingyue Wang; Qing Xiao; Xieyang Wang. The SOC estimation of power Li-Ion battery based on ANFIS model. Smart Grid and Renewable Energy 2012, 3(1), 51-55. [CrossRef]
15. Balci; Selami; Ahmet Kayabasi; Berat Yildiz. ANFIS based voltage determination for photovoltaic systems according to the specific cell parameters, and a simulation for the non-isolated high gain DC-DC boost converter control regard to voltage fluctuations. Applied Solar Energy 2019, 55(6), 357-366. [CrossRef]

ABOUT THE AUTHORS

Kanhu Charan Bhuyan, received his B.Tech. degree in Electronics and Instrumentation Engineering from College of Engineering and Technology (affiliated to Biju Patnaik University of Technology), Odisha, India in 2003 and his M.Tech. degree in Control and Automation specialization from IIT, Delhi, India in 2005. He received his Ph.D. degree from NIT, Rourkela, India in 2014. He is currently working as an Associate Professor at Electronics and Instrumentation department, Odisha University of Technology and Research, Bhubaneswar. His current research interests include digital VLSI, IoT, modeling of photovoltaic cell, fuel cell and control strategies of various power converter and renewable power generation systems.

Pushpak Jain, received the B.Tech. degree in Electrical Engineering from Parla Maharaja Engineering College (Affiliated to BPUT), Berhampur, Odisha, India in 2017 and M.Tech. degree in Electronics and Instrumentation specialization from College of Engineering and Technology (Autonomous), Bhubaneswar, Odisha, India in 2020. He is currently working as a Assistant Professor in Electrical Engineering dept. in Sanskriti University, Chatta Rural, Uttar Pradesh. His current research interests include microgrid, inverter, power converter, renewable energy.

Srutisagar Pattanaik, received the B.Tech. degree in Electronics and Instrumentation Engineering from College of Engineering and Technology (Affiliated to BPUT), Bhubaneswar, Odisha, India in 2017 and M.Tech. degree in Electronics and Instrumentation specialization from College of Engineering and Technology (Autonomous), Bhubaneswar, Odisha, India in 2020. He is currently working as a faculty in Electronics and Instrumentation dept. in Odisha University of Technology and Research, Bhubaneswar. His current research interests include modelling and control of renewable energy systems and various nonlinear systems.